Front. Optoelectron. 2014, 7(1): 77–83
DOI 10.1007/s12200-014-0393-7

RESEARCH ARTICLE

Edge effect of optical surfacing process with different data extension algorithms

Yang LIU[1], Haobo CHENG (✉)[1], Zhichao DONG[1], Hon-Yuen TAM[2]

1 School of Optoelectronics, Beijing Institute of Technology, Beijing 100081, China
2 Department of Mechanical and Biomedical Engineering, City University of Hong Kong, Hong Kong, China

Abstract This study presents a strategy which integrates extra polishing path (EPP) and error map extension to weaken the edge effect in the ultraprecise optical surfacing process. Different data extension algorithms were presented and analyzed. The neighbor-hood average can be selected as the frequently-used method, as it has not bad precision and time-saving performance for most surface forms through the simulation results and practical experiment. The final error map was obtained, its peak-to-valley (*PV*) was 0.273λ and root mean square (*RMS*) was 0.028λ (λ = 632.8 nm). The edge effect was weakened and suppressed well through the experiment.

Keywords edge effect, convergence rate, extension algorithms

1 Introduction

The demands for an efficient workpiece edge figuring process have been increased due to the popularity of segmented optics in many next generation optical systems [1,2]. According to the theoretical basis for wear prediction provided by Preston in 1927, the tool influence function (TIF) is related to the pressure distribution, motion velocity and other parameters, and can remain invariant in the total polishing run time as long as the tool stays inside the workpiece. However, once the tool overhangs the edge of workpiece, the measured TIF tends to make great difference in both the peak removal rate and shape from the nominal behavior due to dramatically varying pressure range, tool bending, and nonlinear effects caused by tool material flow [3]. Thus, one of the most difficult problems in deterministic optical surfacing process is how to figure the edge.

Received December 2, 2013; accepted December 20, 2013

E-mail: chenghaobo@tsinghua.org.cn

Many researches about the edge effect have been presented and developed at home and abroad. Jones [4] suggested a linear pressure distribution model and the orbital tool motion in computer controlled polishing with small tools figuring in 1986. And Zhang et al. [5] presented the modified function of dwell time (e.g., increasing the dwelling time) to improve the edge removal profile. Luna-Aguilar et al. [6] and Cordero-Dávila et al. [7] pointed out a nonlinear pressure distribution (between the tool and the workpiece), like a skin effect near the edge-side of the workpiece which avoided the negative pressure problem well. Furthermore, Kim et al. [3] provided a new parametric model based on measured data by redefining the Preston coefficient, which is always regarded as a universal constant. Wang et al. [8] discussed the force between the molecules of the grinding compound carrier, which have great influence on edge effect in optical processing.

In this paper, an effective edge effect suppression strategy was proposed with extra polishing path (EPP), TIFs and surface error map extensions. The advantages of the strategy are that the TIF used in one polishing run keeps invariant all over the polishing region and the initial residual error map should be extended to ensure that the map could match datum of polishing dwell points exceeding the border owing to the EPP strategy. Then four error map extension algorithms including setting zero [9], Gaussian extension [9,10] neighborhood average extension [11] and Gerchberg-pupil extension [12–14] were investigated in detail. At last, the surface forms with low and high edge gradient were discussed to evaluate the performance of extension algorithms due to the edge gradient affecting the convergence rate of surface form.

2 Data extension algorithms

As mentioned above, the initial surface error map should

be extended. And the extension algorithms make a difference to the convergence of final surface error map. Additionally, the fabrication workpiece are circular or non-regular, the discretized matrix of surface error function would not be filled completely, and the incomplete datum is replaced with NAN (i.e., not a number). This difference can induce an algorithm edge effect and affect the convergence of the iterative algorithm. Edge extensions can weaken or even eliminate this effect.

2.1 Setting zero

The extension by setting zero is the simplest way for the edge extension data. To ensure the extended points' surface error is zero, the dwell time at the edge of the workpiece by deconvolution must be much less than the ideal value. Accordingly, the real material removal must be much less than the ideal, namely there is severe edge effect in the ring where points are with greater surface error.

2.2 Gaussian extension

Gaussian extension is a type of commonly used method. Take an example of a circle mirror with diameter of D, as shown in Fig. 1(a), and the radius of removal function is R_E. And there are three sections in the figure, which are origin valid data region, a circle extended valid region with the diameter of $D+2R_{\mathrm{E}}$, and a square extended matrix with the width of $D+2R_{\mathrm{E}}$. With the Gaussian extension, the surface error value of any point B in the extended area can be expressed as Eq. (1)

$$E(\mathrm{B}) = E(\mathrm{A})\exp\left(-\frac{l^2}{2\sigma^2}\right), \tag{1}$$

where σ is the parameter of Gaussian extension, generally selected $\sigma \geqslant R_{\mathrm{E}}/3$; B is the point to be extended; A is the edge point of origin valid data region in the radial direction of point B at the same time; l is the distance between the extended point B and edge point A. The errors of points A, B, C are shown in Fig. 1(a).

It is reasonable to extend the origin data with Gaussian function, if the removal function used is Gaussian shape. Simultaneously, the Gaussian function has perfect smoothing effect and can lower the mutability of dwell time located at the edge in deconvolution. However, there is a serious weakness with Gaussian extension that the surface figure is carried out just based on the surface figure of one point which is at the edge of the radial direction, thus it cannot completely deliver the messages of all points involved in convolution. What's more, if the reference point is "noise" (whose surface figure is distinctively different from points around it), the extension result will become worse. So Gaussian extension could not cope with complex edge data, and its practical application is limited.

2.3 Neighborhood extension

Take an example of a circle mirror with diameter of D about the neighborhood extension method, as shown in Fig. 2, and the radius of removal function is R_{E}. The data connectivity should be ensured to improve the smoothness and continuity of extension. Thus if and only if there are at least three valid data points around the eight neighborhood points of the extension point, the edge extension can be calculated. As shown in Fig. 2, the points A and B are conformed with the above principle, not the point C.

In this paper, the center of the surface error map is considered as the initial point. Then the total surface is divided into four quadrants, in every which the nearest point to initial point is analyzed first and other points are analyzed sequentially along two directions. As shown in Fig. 2, for example in one quadrant, the black dot is

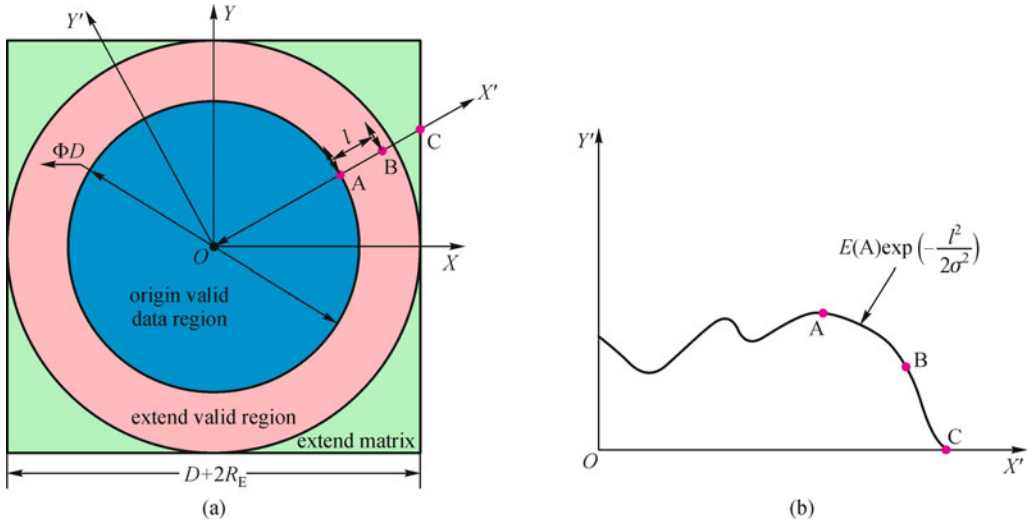

Fig. 1 Schematic diagram of Gaussian extension method

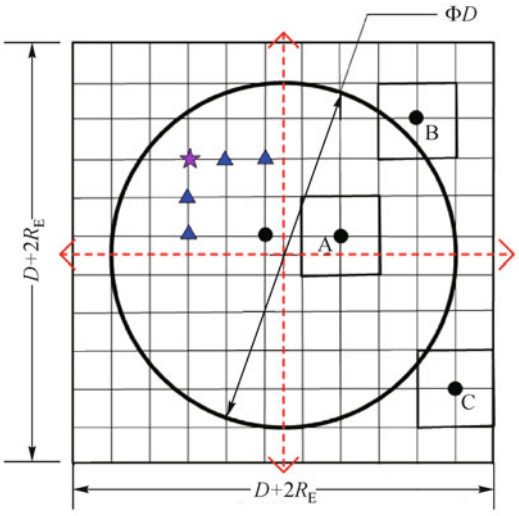

Fig. 2 Schematic diagram of neighborhood extension method

regarded as the first analysis point, and then the points are analyzed like the blue triangle along the two directions, horizontally and vertically, at last, the point of intersection of two directions is analyzed like the pink pentagram. In this way, the calculation rate is improved greatly.

2.4 Gerchberg-pupil extension

Gerchberg-pupil extension, also called Gerchberg bandlimited extrapolation algorithm, is used to extend the factual surface error map in two dimensions. And here, Gerchberg's 1-D iterative extrapolation algorithm for bandlimited signals is introduced first. Here, $u(x)$ denotes the initial surface error map that is nonzero over region T_x, the extended region is denoted by T_{x0}. And $H = (G_{T_{x0}} - G_{T_x})F^{-1}G_{\Omega_{f_x}}F$ is the extension operator, F and F^{-1} are Fourier transform and Fourier inverse transform.

The final surface error map $u_N(x)$ after iterative extension is expressed as (Eq. (2))

$$u_N(x) = \sum_{n=0}^{N} H^n u(x) G_{T_{x0}}, \tag{2}$$

where the initial and extended surface region aperture are expressed separately by

$$G_{T_x} = \begin{cases} 1, & x \in T_x, \\ 0, & x \notin T_x, \end{cases} \quad G_{T_{x0}} = \begin{cases} 1, & x \in T_{x0}, \\ 0, & x \notin T_{x0}. \end{cases} \tag{3}$$

Similarly, $\Omega_{f_x f_y}$ is defined the bandlimited spectrum, and correspondingly, the spectral pupil is

$$G_{\Omega_{f_x}} = \begin{cases} 1, & x \in \Omega_{f_x}, \\ 0, & x \notin \Omega_{f_x}. \end{cases} \tag{4}$$

It has been proved that $u_N(x)$ will converge to $u(x)$ with bandlimited region Ω_{f_x} as $N \to \infty$. In engineering, Eq. (2) is run to some N to ensure a smooth joint at the edge through fast Fourier transform.

The steps of Gerchberg-pupil extension above are summed up as follows:

1) Extend the origin region T_x to extended regionT_{x0};
2) Fourier transform $F\left(u(x)G_{T_{x0}}\right)$;
3) Truncate the spectrum through multiplying by $G_{\Omega_{f_x}}$;
4) Then Fourier inverse transform;
5) Discard that portion where the signal is known by multiplying by $(G_{T_{x0}} - G_{T_x})$;
6) Add in the known signal $u(x)G_{T_{x0}}$;
7) Fourier transform for the last equation, go to step 3, and repeat.

Figure 3 shows the result of the Gerchberg's 1-D algorithm. The edge extension in Fig. 3(a) is enlarged in Fig. 3(b). The elliptical regions denoted in Fig. 3 are indicated the extension region and the result after extension. As can be seen in Fig. 3, the origin region without the zero region is $(-\pi,\pi)$, and the region after

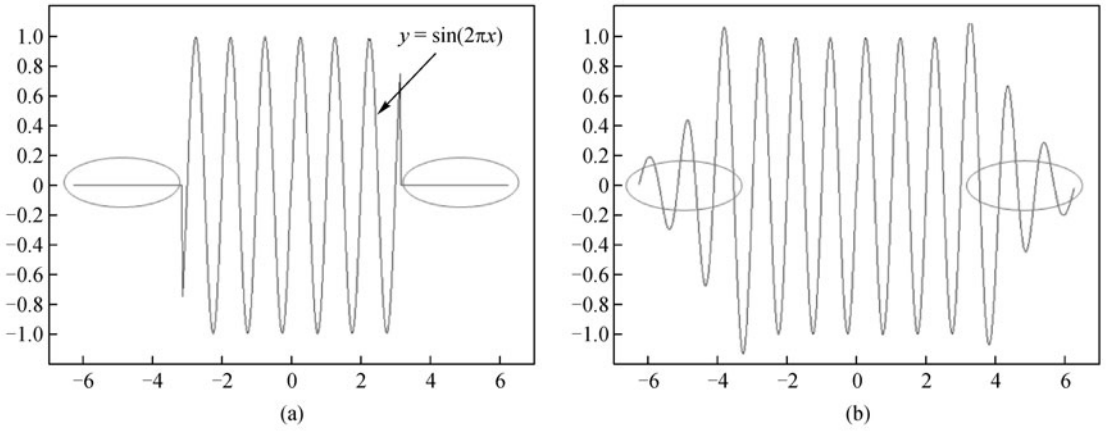

Fig. 3 Results with Gerchberg's 1-D algorithm. (a) Initial data; (b) data after extended

extended is $(-2\pi,2\pi)$. The result shows that the extension is relative continuity and smoothness.

In the practical engineering, Gerchberg's 1-D algorithm is extended to Gerchberg's 2-D algorithm, Gerchberg-pupil extension, for the extrapolation extension of origin surface error map. Here, $u(x,y)$ denotes the initial surface error map that is nonzero over region T_{xy}, the extended region is denoted by T_{xy0}, the extra expansion region is set by zero. And $u(f_x,f_y)$ is the Fourier transform $F\left(u(x,y)G_{T_{xy0}}\right)$, its bandlimited domain is $\Omega_{f_xf_y}$. $G_{T_{xy}}$, $G_{T_{xy0}}$, $G_{\Omega_{f_xf_y}}$ are unit functions of region T_{xy}, T_{xy0}, $\Omega_{f_xf_y}$, respectively. So the $u(x,y)$ extended is expressed as (Eq. (5))

$$u_N(x,y) = \sum_{n=0}^{N} H^n u(x,y) G_{T_{xy0}}. \tag{5}$$

Similarity of Gerchberg's 1-D algorithm, here $H = (G_{T_{xy0}} - G_{T_{xy}})F^{-1}G_{\Omega_{fxfy}}F$ is the extension operator. It has also been proved that $u_N(x,y)$ will converge to $u(x,y)$ with bandlimited region $\Omega_{f_xf_y}$ as $N \to \infty$.

3 Experiments for evaluation of performance

3.1 Error map with low edge gradient

The simulation initial surface with low edge gradient is $PV = 0.665\lambda$ (PV: peak-to-valley), and $RMS = 0.13920\lambda$ (RMS: root mean square). The outermost edge gradient datum is extracted to figure out the edge gradient $RMS = 17.2359$.

The four extension methods mentioned above are respectively used to the surface error with low edge gradient shown in the Fig. 4. The origin surface form in Fig. 4(a) is inside the red solid line, three others just the same. The extension results are obvious to be seen that the Gerchberg-pupil extension is best and smoothest, neighborhood extension is second and setting zero is worst and of the great saltation.

3.2 Error map with high edge gradient

The surface with high edge gradient is $PV = 0.611\lambda$ and $RMS = 0.12468\lambda$, and the outermost edge gradient datum are $RMS = 123.8224$.

The four extension methods mentioned above are respectively used to the surface error with high edge gradient in Fig. 5. The origin surface form in Fig. 5(a) is inside the red solid line, three others just the same. The extension results are obvious to be seen that the Gerchberg-pupil extension is the best and smoothest, neighborhood extension is second and setting zero is worst and of the great saltation. The red rectangle marks indicate the great saltation which is obvious to be seen in Figs. 5(b) and 5(c). Compared to surface form with low edge gradient, the results of Gaussian extension and neighborhood average are limited for surface form with high edge gradient.

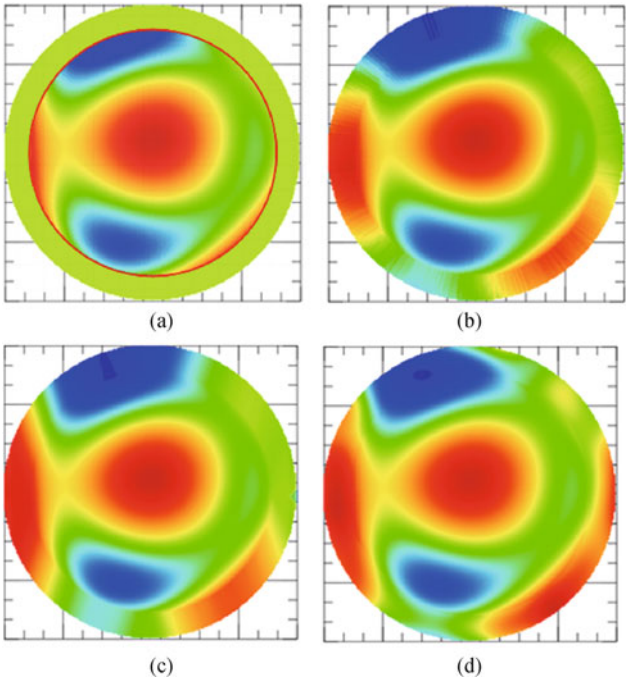

Fig. 4 Schematic diagrams with different extension methods (with low edge gradient). (a) Setting zero; (b) Gaussian extension; (c) neighborhood extension; (d) Gerchberg-pupil extension

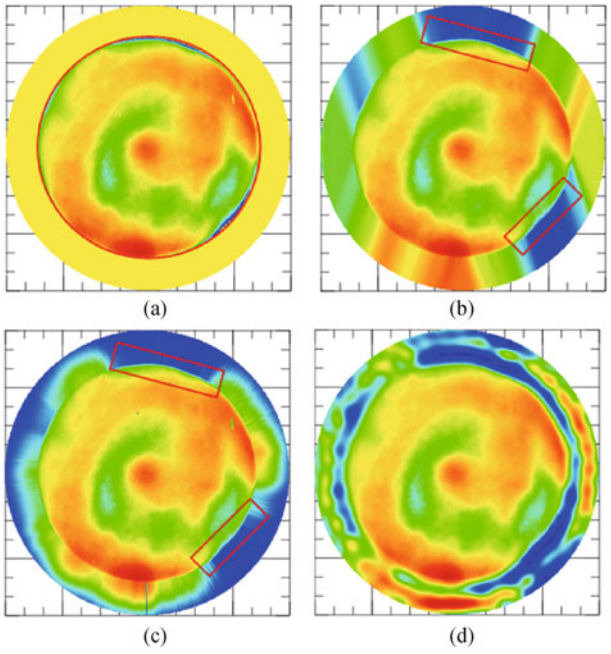

Fig. 5 Schematic diagrams with different extension methods (with high edge gradient). (a) Setting zero; (b) Gaussian extension; (c) neighborhood extension; (d) Gerchberg-pupil extension

3.3 Influences on convergence rate

The simulations were made to evaluate the different extension in Fig. 6. Figure 6(a) is about *PV* and *RMS* comparison of surface form with low and high edge gradient. And Fig. 6(b) is about convergence rate comparison of surface form with low and high edge gradient. According to Fig. 6, the convergence rate of setting zero is the worst, and the neighborhood extension ranks only second to the best Gerchberg-pupil extension. However, the extension time of Gerchberg-pupil is longest. It takes 22.5 s for the low edge gradient to extend origin data and 280 s for the high edge gradient. Other three extensions are saving-time about 0.2 s.

3.4 Experiment

We performed an experiment using magnetorheological finishing (MRF) on a Φ 100 mm plane work-piece with evident edge effect and initial surface error map: $PV = 0.805\lambda$, $RMS = 0.161\lambda$, as shown in Fig. 7(a).

The abrasive is composed of cerium oxide, carbonyl iron powder, silicone oil according to certain proportion and its peak removal rate is 0.5λ/min in our MRF equipment. The paths of concentric circles and Hilbert were taken in the polishing process. The each total fabrication points and the extension edge range using neighborhood extension were depended on the last fabrication result. The total process takes four and a half hours in two fabrication stage. The first stage is three hours and the second stage one and a half hours. After the iterative fabrications, we obtained the final surface error shape: $PV = 0.170\lambda$, $RMS = 0.019\lambda$ as shown in Fig. 7(b). We can see that the edge effect was

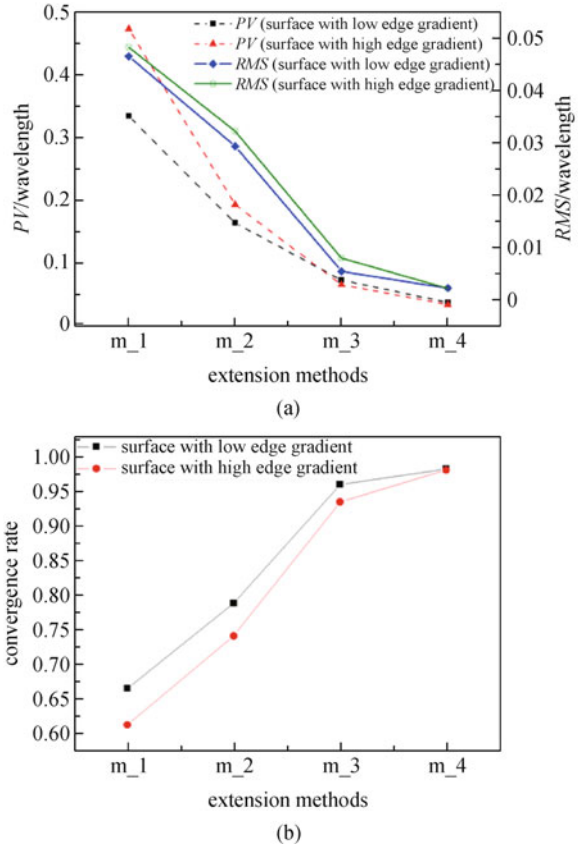

Fig. 6 Results comparison of surface forms with low and high edge gradients with different extensions. (a) Results of *PV* and *RMS*; (b) results of convergence rate (m_1: setting zero; m_2: Gaussian extension; m_3: neighborhood extension; m_4: Gerchberg-pupil extension)

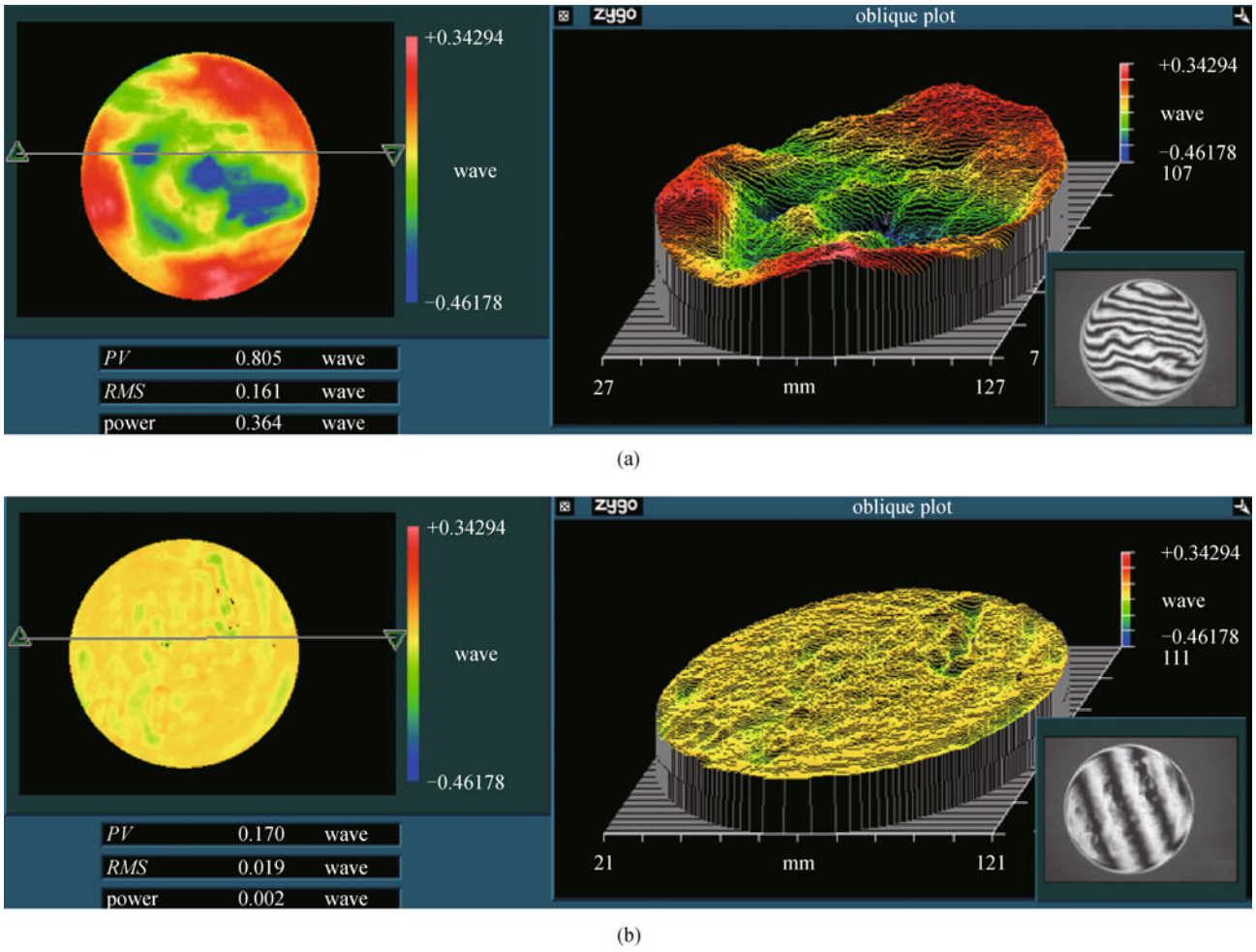

Fig. 7 Surface error map. (a) Initial surface error map: $PV = 0.805\lambda$, $RMS = 0.161\lambda$; (b) final surface error map: $PV = 0.170\lambda$, $RMS = 0.019\lambda$

weakened and suppressed well through the experiment. It is proved that the neighborhood extension has good influence on the edge effect.

4 Conclusions

In this paper, a suppression strategy was discussed by utilizing extra polishing path and TIFs without edge effect and advance dwell time algorithm. Several data extension algorithms including setting zero, Gaussian extension, neighborhood average and iterative Gerchberg-Pupil extension were theoretically researched to obtain an ideal solution to suppress the edge effect. Simulation results show that setting zero method results in great saltation of edge data, which highly reduces the convergence rate; Gaussian extension could not cope with complex edge data, and its practical application is limited; the Gerchberg-Pupil extension has superior convergent precision, especially suitable to high gradient edge region, but it may takes long time for its hundreds of iterative FFT process; neighbor-hood average could be selected as the frequently-used method as it has no bad precision and time-saving performance for common error map. The experiment obtaining the final surface error shape 0.273λ (PV) and 0.028λ (RMS) also indicates that the neighborhood extension has good influence on the edge effect.

Acknowledgements This work was supported by the Research Grants Council of the Hong Kong Special Administrative Region (No. CityU 120610).

References

1. Johns M. The giant magellan telescope (GMT). In: Proceedings of SPIE, Extremely Large Telescopes: Which Wavelengths? Lund, Sweden, 2008, 6986: 696803-1–696803-12
2. Clampin M. Status of the James Webb space telescope (JWST). In: Proceedings of SPIE, Astronomical Telescopes and Instrumentation: Synergies Between Ground and Space. France, 2008, 7010: 70100L-1–70100L-7
3. Kim D W, Park W H, Kim S W, Burge J H. Parametric modeling of

edge effects for polishing tool influence functions. Optics Express, 2009, 17(7): 5656–5665
4. Jones R A. Computer-controlled optical surfacing with orbital tool motion. Optical Engineering (Redondo Beach, Calif.), 1986, 25(6): 785–790
5. Zhang X J, Yu J C, Sun X F. Theoretical method for edge figuring in computer-controlled polishing of optical surface. In: Proceedings of SPIE's 1993 International Symposium on Optics, Imaging, and Instrumentation. 1994, 239–246
6. Luna-Aguilar E, Cordero-Davila A, Gonzalez J, Nunez-Alfonso M, Cabrera V, Robledo-Sanchez C I, Cuautle-Cortez J, Pedrayes M H. Edge effects with Preston equation. In: Procedings of SPIE, Astronomical Telescopes and Instrumentation. 2003, 4840: 598–603
7. Cordero-Dávila A, González-García J, Pedrayes-López M, Aguilar-Chiu L A, Cuautle-Cortés J, Robledo-Sánchez C. Edge effects with the Preston equation for a circular tool and workpiece. Applied Optics, 2004, 43(6): 1250–1254
8. Wang T, Cheng H B, Feng Y P, Dong Z C. Simulation analysis of edge effect in typical processing. Transactions of Beijing Institute of Technology, 2011, 31(9): 1100–1103
9. Shu L X, Wu F, Shi C Y. Optimization of the edge extension in dwell time algorithm for ion beam figuring. In: Proceedings of 6th International Symposium on Advanced Optical Manufacturing and Testing Technologies (AOMATT). 2012, 8416: 84162M-1–84162M-6
10. Jiao C J, Li S Y, Xie X H. Algorithm for ion beam figuring of low-gradient mirrors. Applied Optics, 2009, 48(21): 4090–4096
11. Zhou L. Optical mirror ion beam figuring theory and technology. Dissertation for the Doctoral Degree. Hunan: National University of Defense Technology, 2008, 30–43 (in Chinese)
12. Wu J. Research on ion beam figuring technology. Dissertation for the Doctoral Degree. Jilin: Changchun Institute of optics, Fine Mechanics and Physics, Chinese Academy of Science, 2010, 13–38
13. Marks II R J. Gerchberg's extrapolation algorithm in two dimensions. Applied Optics, 1981, 20(10): 1815–1820
14. Wu J F, Lu Z W, Zhang H X, Wang T S. Dwell time algorithm in ion beam figuring. Applied Optics, 2009, 48(20): 3930–3937

Yang Liu is a current Master student at Beijing Institute of Technology and she received her Bachelor degree at Dalian Nationalities University in 2011. Her current research is in the area of optical processing and testing.

Haobo Cheng is a current Professor Doctoral supervisor in Beijing Institute of Technology. He received his Ph.D degree in Changchun Institute of Optics, Fine Mechanics and Physics, Chinese Academy of Sciences. He is also the dean of research institute in Zhuhai and director at the joint research center for opto-mechatronics engineering. The present research work is precision ultra-precision manufacturing and testing.

Zhichao Dong is a doctor at Beijing Institute of Technology where he also got his Master degree. And he received his Bachelor degree at Qingdao University. He engaged in the fabrication of an off-axis aspherical mirror with a lager-aperture.

Hon-Yuen TAM obtained his B.Sc from Georgia Institute of Technology, M.Sc and Ph.D from Stanford University, all in Mechanical Engineering. He is a Chartered Engineer and a fellow of the Institution of Measurement and Control, UK. He is a University Lecturer in City University of Hong Kong and his research interest is Surface finishing automation and in numerical control.